

σ and $f_0(980)$ substructures from $\gamma\gamma \rightarrow \pi\pi, J/\psi, \phi$ radiative and D_s semi-leptonic decays

G. Mennessier^a, S. Narison^{a,*}, X.-G. Wang^{a,b,**}

^aLaboratoire de Physique Théorique et Astroparticules, CNRS-IN2P3, Case 070, Place Eugène Bataillon, 34095 - Montpellier Cedex 05, France.

^bDepartment of Physics, Peking University, Beijing 100871, China.

Abstract

Using an improved “analytic K -matrix model”, we reconsider the extraction of the $\sigma \equiv f_0(600)$ and $f_0(980)$ $\gamma\gamma$ widths from $\gamma\gamma \rightarrow \pi\pi$ scatterings data of Crystal Ball and Belle. Our main results are summarized in Tables 3 and 4. The averaged σ “direct width” to $\gamma\gamma$ is $0.16(3)$ keV which confirms a previous result of [1] and which does neither favour a large four-quark (diquark-antidiquark) or a molecule nor a pure $\bar{q}q$ components. The “direct width” of the $f_0(980)$ of $0.28(2)$ keV is much larger than the four-quark expectation but can be compatible with a $\bar{s}s$ or gluonium component. We also found that the rescattering part of each amplitude is relatively large indicating an important contribution of the meson loops in the determinations of the σ and $f_0(980)$ $\gamma\gamma$ total widths. This is mainly due to the large couplings of the σ and $f_0(980)$ to $\pi\pi$ and/or $\bar{K}K$, which can also be due to a light scalar gluonium with large OZI violating couplings but not necessary to a four-quark or molecule state. Our average results for the total (direct+rescattering) $\gamma\gamma$ widths: $\Gamma_{\sigma}^{tot} = 3.08(82)$ keV, $\Gamma_{f_0}^{tot} = 0.16(1)$ keV are comparable with the ones from dispersion relations and PDG values. Using the parameters from QCD spectral sum rules, we complete our analysis by showing that the production rates of unmixed scalar gluonia $\sigma_B(1)$ and G (1.5-1.6) agree with the data from $J/\psi, \phi$ radiative and D_s semi-leptonic decays.

Keywords:

$\gamma\gamma$ and $\pi\pi$ scatterings, radiative decays, light scalar mesons, gluonia and four-quark states, QCD spectral sum rules and low-energy theorems.

1. Introduction

In previous series of papers [1–3], we have used an improved version of the K -matrix model originally proposed in [4] for studying the hadronic and $\gamma\gamma$ couplings of the $\sigma/f_0(600)$ meson¹. We found that the “direct” coupling of the σ to $\gamma\gamma$ is more compatible with a large gluon component in its wave function rather than with a $\bar{q}q$ (too large $\gamma\gamma$ width) or four-quark (too small $\gamma\gamma$ width). More recently, we have extended the analysis for studying the hadronic couplings of the $\sigma/f_0(600)$ and $f_0(980)$ mesons [2, 3]. We found an unexpected relatively large coupling of the σ to $\bar{K}K$: $|g_{\sigma K^+ K^-}|/|g_{\sigma\pi^+\pi^-}| = 0.37(6)$ ², which disfavours its large $\pi - \pi$ molecule and four-quark components, while the large coupling of $f_0(980)$ to $\bar{K}K$: $|g_{f_0 K^+ K^-}|/|g_{f_0\pi^+\pi^-}| = 2.59(1.34)$, excludes its pure ($\bar{u}u + \bar{d}d$) content. These phenomenological observations go in lines with the fact that, in the $I = 0$ channel, the gluon component is expected to play an essential rôle through the scalar QCD anomaly (dilaton) [10–19] which manifests through the trace of the QCD energy momentum tensor:

$$\theta_{\mu}^{\mu} = \sum_{i=u,d,s} m_i (1 + \gamma_m) \bar{\psi}_i \psi_i + \frac{1}{4} \beta(\alpha_s) G^2, \quad (1)$$

^{*}Corresponding author

^{**}China scholarship council fellow under contract n° 2009601139.

Email addresses: gerard.mennessier@lpta.univ-montp2.fr (G. Mennessier), snarison@yahoo.fr (S. Narison), wangxuangan@pku.edu.cn (X.-G. Wang),

¹Some other applications of the model have been discussed in [5, 6].

²Analogous values have been obtained in [4, 7, 8] and in Fits 9 and 10 of [9] though not favoured by [9].

where γ_m is the quark mass anomalous dimension; ψ_i is the quark field; $\beta(\alpha_s)$ is the Gell-Mann-Low QCD β -function and G^2 is the gluon field strength.

In this paper, we pursue the test of the nature of these scalar mesons by studying their couplings to $\gamma\gamma$ inside the energy region below 1.4 GeV, where new data on $\gamma\gamma \rightarrow \pi\pi$ from BELLE [20] is available in addition to the old data of Crystal Ball [21] and MARK II [22].

2. The analytic K -matrix model for $\pi\pi \rightarrow \pi\pi/\bar{K}K$

In this approach, the strong processes are described by a K -matrix model representing the amplitudes by a set of resonance poles [4] and where the dispersion relations in the multi-channel case can be solved explicitly. The model can be reproduced by a set of Feynman diagrams, including resonance (bare) couplings to $\pi\pi$ and $\bar{K}K$ and (in the original model [4]) 4-point $\pi\pi$ and $\bar{K}K$ interaction vertices which we shall omit for simplicity in [1] and here. A subclass of bubble pion loop diagrams including resonance poles in the s-channel are resummed (unitarized Born). In a previous work [3], we have discussed the approach for the case of : 1 channel \oplus 1 “bare” resonance (K -matrix pole) and 2 channels \oplus 2 “bare” resonances and we have restricted to the $SU(3)$ symmetric shape function. We have introduced a real analytic form factor *shape function*, which takes explicitly into account left-handed cut singularities for the strong interaction amplitude, and which allows a more flexible parametrisation of the $\pi\pi \rightarrow \pi\pi/\bar{K}K$ data. In our low energy approach, the shape

function can be conveniently approximated by³:

$$f_P(s) = \frac{s - s_{AP}}{s - \sigma_{DP}}, \quad P \equiv \pi, K, \quad (2)$$

which multiplies the scalar meson couplings to $\pi\pi/\bar{K}K$. In this form, the *shape function* allows for an Adler zero at $s = s_{AP}$ and a pole for $\sigma_{DP} < 0$ simulating the left hand cut.

• 1 channel \oplus 1 “bare” resonance

Let's first illustrate the method in this simple case. The unitary PP amplitude is then written as:

$$T_{PP}(s) = \frac{G_P f_P(s)}{s_R - s - G_P \tilde{f}_P(s)} = \frac{G_P f_P(s)}{\mathcal{D}_P(s)}, \quad (3)$$

where $T_{PP} = e^{i\delta_P} \sin \delta_P / \rho_P(s)$ with $\rho_P(s) = (1 - 4m_P^2/s)^{1/2}$; $G_P = g_{\sigma P, B}^2$ are the bare coupling squared and :

$$\text{Im } \mathcal{D}_P = \text{Im } (-G_P \tilde{f}_P) = -(\theta \rho_P) G_P f_P, \quad (4)$$

with: $(\theta \rho_P)(s) = 0$ below and $(\theta \rho_P)(s) = \rho_P(s)$ above threshold $s = 4m_P^2$. The “physical” couplings are defined from the residues, with the normalization:

$$g_{\sigma P}^2 \equiv g_{\sigma PP}^2 / (16\pi) : \quad \Gamma_{\sigma \rightarrow \pi\pi} = \frac{|g_{\sigma PP}(M_\sigma^2)|^2}{16\pi M_\sigma} \rho_P(M_\sigma^2). \quad (5)$$

The amplitude near the pole s_0 where $\mathcal{D}_P(s_0) = 0$ and $\mathcal{D}_P(s) \approx \mathcal{D}'_P(s_0)(s - s_0)$ is:

$$T_{PP}(s) \sim \frac{g_{\sigma P}^2}{s_0 - s}; \quad g_{\sigma P}^2 = \frac{G_P f_P(s_0)}{-\mathcal{D}'_P(s_0)}. \quad (6)$$

The real part of \mathcal{D}_P is obtained from a dispersion relation with subtraction at $s = 0$ and one obtains:

$$\tilde{f}_P(s) = \frac{2}{\pi} \left[h_P(s) - h_P(0) \right], \quad (7)$$

with: $h_P(s) = f_P(s) \tilde{L}_{s1}(s) - (\sigma_{NP}/(s - \sigma_{DP})) \tilde{L}_{s1}(\sigma_{DP})$, σ_{NP} is the residue of $f_P(s)$ at σ_{DP} and: $\tilde{L}_{s1}(s) = \left[(s - 4m_P^2)/m_P^2 \right] \tilde{L}_1(s, m_P^2)$ where: \tilde{L}_1 from [4].

• Generalization to 2 channels \oplus 2 “bare” resonances

In [2, 3], we have generalized the previous case to the one of 2 channels \oplus 2 “bare” resonances.

3. The $\gamma\gamma \rightarrow \pi\pi$ process

• Expression and normalization of the amplitudes

The amplitude $\gamma(q_1, \epsilon_1) + \gamma_2(q_2, \epsilon_2) \rightarrow \pi(p_1) + \bar{\pi}(p_2)$ of mass m_π can be written in terms of the invariants⁴:

$$\begin{aligned} A &= I_1 A_1 + I_2 A_2, \\ I_1 &= (\epsilon_1 \cdot \epsilon_2) - (\epsilon_1 \cdot q_2)(\epsilon_2 \cdot q_1)/(q_1 \cdot q_2), \\ I_2 &= (\epsilon_1 \cdot \Delta)(\epsilon_2 \cdot \Delta)(q_1 \cdot q_2) - (\epsilon_1 \cdot q_2)(\epsilon_2 \cdot \Delta)(q_1 \cdot \Delta) \\ &\quad - (\epsilon_2 \cdot q_1)(\epsilon_1 \cdot \Delta)(q_2 \cdot \Delta) \\ &\quad + (\epsilon_1 \cdot q_2)(\epsilon_2 \cdot q_1)(q_1 \cdot \Delta)(q_2 \cdot \Delta)/(q_1 \cdot q_2), \end{aligned} \quad (8)$$

with $\Delta = p_1 - p_2$. Helicity $\lambda = 0$ and $\lambda = 2$ amplitudes are denoted by F and G , which, in terms of partial wave amplitudes, read respectively:

$$\begin{aligned} F &= A_1 - s(s/4 - m_\pi^2) \sin^2 \theta A_2 \\ &= \sum_{\text{even } J \geq 0} (2J+1) f^{J0}(s) d_{00}^J(\theta), \\ G &= s(s/4 - m_\pi^2) \sin^2 \theta A_2 \\ &= \sum_{\text{even } J \geq 2} (2J+1) g^{J2}(s) d_{20}^J(\theta) 4/\sqrt{6}. \end{aligned} \quad (9)$$

d_{20}^J and d_{00}^J are the usual d -functions normalized as in PDG [23], while θ is the scattering angle between \vec{p} and \vec{q} , which can be expressed in terms of s and t as:

$$\cos \theta = \frac{2t + s - 2m_\pi^2}{\sqrt{s(s - 4m_\pi^2)}}. \quad (10)$$

For unpolarized photons, the cross section reads:

$$\frac{d\sigma}{d\Omega} = \frac{2}{s} \sqrt{1 - \frac{4m_\pi^2}{s}} (|F|^2 + |G|^2), \quad (11)$$

where the $\cos \theta$ integration should be done from 0 to 1 for the neutral and from -1 to 1 for the charged cases. In the following analysis, we find convenient to express the charged F_C and neutral F_N amplitudes in terms of the $I = 0$ and $I = 2$ isospin ones⁵:

$$\begin{aligned} F_C &= \sqrt{\frac{2}{3}} \left(F^{I=0} + \frac{1}{\sqrt{2}} F^{I=2} \right), \\ F_N &= -\sqrt{\frac{2}{3}} \left(F^{I=0} - \sqrt{2} F^{I=2} \right). \end{aligned} \quad (12)$$

corresponding to the following $|\pi\pi\rangle$ states:

$$\begin{aligned} |\pi\pi, I=0\rangle &= \sqrt{\frac{2}{3}} \left(|\pi^+ \pi^-\rangle - \frac{1}{2} |\pi^0 \pi^0\rangle \right), \\ |\pi\pi, I=2\rangle &= \sqrt{\frac{1}{3}} \left(|\pi^+ \pi^-\rangle + |\pi^0 \pi^0\rangle \right). \end{aligned} \quad (13)$$

³Here and in the following σ_D is negative and is opposite in sign with the one used in our previous works [1–3].

⁴We use the same normalization as [4].

⁵We use the same convention as [4] where F_C is opposite in sign with [27].

- **The example of one pion exchange for $\gamma\gamma \rightarrow \pi^+\pi^-$**

The expression of the Born term amplitude due to one pion exchange reads ⁶:

$$T_\pi^B = \frac{\alpha}{2} \left[\epsilon_1 \cdot \epsilon_2 - \frac{2(\epsilon_1 \cdot p_1)(\epsilon_2 \cdot p_1)}{t - m_\pi^2} - \frac{2(\epsilon_1 \cdot p_1)(\epsilon_2 \cdot p_1)}{u - m_\pi^2} \right] \quad (14)$$

from which one can deduce the helicity amplitudes:

$$\begin{aligned} F_\pi^B &= \frac{\alpha}{2} \frac{m_\pi^2 s}{(t - m_\pi^2)(u - m_\pi^2)}, \\ G_\pi^B &= \frac{\alpha}{2} \frac{t^2 + ts - 2m_\pi^2 t + m_\pi^4}{(t - m_\pi^2)(u - m_\pi^2)}. \end{aligned} \quad (15)$$

- **Amplitudes for 1 channel \oplus 1 resonance below 0.7 GeV**

– *The isospin $I=0$ channel:* starting from the S wave amplitude in Eq. (3), we derive the amplitude $T_\gamma^{(I)}$ for the electromagnetic process for isospin $I = 0$ as:

$$T_\gamma^{(0)} = \sqrt{\frac{2}{3}} \alpha \left(f_P^B + G_P \frac{\tilde{f}_P^B}{\mathcal{D}_P} \right) + \alpha \frac{\mathcal{P}}{\mathcal{D}_P}. \quad (16)$$

Here the contribution from the Born term of $\gamma\gamma \rightarrow \pi^+\pi^-$ is given by $f_P^B = 2L_1$ as defined in [4], a real analytic function in the s plane with left cut $s \leq 0$. The function \tilde{f}_P^B represents $\pi\pi$ rescattering; it is regular for $s < 4m_\pi^2$ but has a right cut for $s \geq 4m_\pi^2$ with:

$$\text{Im } \tilde{f}_P^B(s + i\epsilon) = (\theta\rho f_P f_P^B)(s), \quad (17)$$

which vanishes at $s = 0$. With this definition the Watson theorem is fulfilled, i.e. the phase of $T_\gamma^{(0)}$ is the same as the one of the elastic amplitude \mathcal{D}_P^{-1} in Eq. (3). The real part is derived from a dispersion relation with subtraction at $s = 0$ for \tilde{f}_P^B to satisfy the Thomson limit, and has a representation similar to the one in Eq. (7), but by replacing (\tilde{f}_P, h_P) by (\tilde{f}_P^B, h_P^B) . The function h_P^B is defined as h_P below Eq. (7) but with \tilde{L}_1 replaced by $-\tilde{L}_1^2$ everywhere. It vanishes at $s = \sigma_{DP}$ and $\tilde{f}_P^B(s)$ is regular at this point. Finally, the polynomial \mathcal{P} reflects the ambiguity from the dispersion relations and is set here to $\mathcal{P} = sF_\gamma \sqrt{2}$. It represents the direct coupling of the resonance to $\gamma\gamma$. The residues at the pole s_0 of the rescattering and direct contributions to $T_\gamma^{(0)}$ in Eq. (16), respectively, are obtained as:

$$g_{\sigma\gamma}^{\text{resc}} g_{\sigma\pi} = \sqrt{\frac{2}{3}} \alpha \frac{G \tilde{f}_P^B(s_0)}{-\mathcal{D}'_P(s_0)}, \quad g_{\sigma\gamma}^{\text{dir}} g_{\sigma\pi} = \alpha \frac{s_0 F_\gamma \sqrt{2}}{-\mathcal{D}'_P(s_0)}, \quad (18)$$

from which one can deduce the branching ratio:

$$\frac{\Gamma_{\sigma \rightarrow \gamma\gamma}}{\Gamma_{\sigma \rightarrow \pi\pi}} \simeq \frac{1}{|\rho(s_0)|} \left| \frac{g_{\sigma\gamma}}{g_{\sigma\pi}} \right|^2 \simeq \frac{2\alpha^2}{|\rho(s_0)|} \left| \frac{s_0}{G f_P(s_0)} \right|^2 F_\gamma^2. \quad (19)$$

– *The isospin $I=2$ channel:* similarly, we parametrize the $I = 2$ S-wave amplitude $T_0^{(2)}$ by introducing the shape function f_2 :

$$T_0^{(2)} = \frac{\Lambda f_2(s)}{1 - \Lambda \tilde{f}_2(s)}, \quad f_2(s) = \frac{s - s_{A2}}{(s - \sigma_{D1})(s - \sigma_{D2})}, \quad (20)$$

⁶Here and in the following, we use the same normalization as in [4] and we use the gauge conditions: $\epsilon_i q_i = \epsilon_i q_j = 0 : i, j = 1, 2$.

and obtain:

$$T_\gamma^{(2)} = \frac{\alpha}{\sqrt{3}} \left(f_2^B + \frac{\Lambda \tilde{f}_2^B(s)}{1 - \Lambda \tilde{f}_2(s)} \right), \quad (21)$$

where $f_2^B = f_P^B$ and: $\text{Im } \tilde{f}_2(s) = (\theta\rho f_2(s))$, $\text{Im } \tilde{f}_2^B(s) = (\theta\rho f_2 f_P^B)(s)$. These amplitudes are again both subtracted at $s = 0$ as in case of $I = 0$ and one finds in analogy:

$$\tilde{f}_2(s) = \frac{2}{\pi} \left[h_2(s) - h_2(0) \right], \quad (22)$$

where: $h_2(s) = f_2(s) \tilde{L}_{s1}(s) - (\sigma_{N1}/(s - \sigma_{D1})) \tilde{L}_{s1}(\sigma_{D1}) - (\sigma_{N2}/(s - \sigma_{D2})) \tilde{L}_{s1}(\sigma_{D2})$; σ_{N1}, σ_{N2} are the residues of $f_2(s)$ at σ_{D1}, σ_{D2} and $\tilde{f}_2^B(s)$ is defined as $\tilde{f}_2(s)$ in Eq. (22) but with \tilde{L}_1 replaced by $-\tilde{L}_1^2$. The cross sections for the $\pi\pi$ and $\gamma\gamma$ scattering processes are obtained from the previous expressions of the amplitudes.

- **Results of the analysis**

In doing the analysis for the case of elastic $\pi\pi \rightarrow \pi\pi$ scattering and $\gamma\gamma \rightarrow \pi\pi$ below 700 MeV where the Crystal Ball [21] and MARK II [22] data have been used, we have obtained in [1] the results summarized in Table 4.

4. Extension of the $\gamma\gamma \rightarrow \pi\pi$ analysis below 1.09 GeV

In this paper, we extend the previous analysis by including $\pi\pi$ and $\bar{K}K$ loops and work in the region just above the $\bar{K}K$ threshold (the minimal χ^2/ndf of our fit is obtained for $\sqrt{s} = 1.09$ GeV), where the $\sigma(600)$, $f_0(980)$ contributions are dominant.

• S-waves masses and hadronic couplings

In this case with 2 resonances \oplus 2 channels, the hadronic masses and couplings of the $\sigma(600)$ and $f_0(980)$ and the corresponding values of the “bare parameters” of the model are given in Tables 2 and 3 of [3] which we shall use in the extraction of their $\gamma\gamma$ couplings. The values of the masses are (in units of MeV):

$$M_\sigma = 452(12) - i260(15), \quad M_f = 981(34) - i18(11), \quad (23)$$

and the ratios of the hadronic couplings are:

$$\frac{|g_{\sigma K^+ K^-}|}{|g_{\sigma \pi^+ \pi^-}|} = 0.37(6), \quad \frac{|g_{f K^+ K^-}|}{|g_{f \pi^+ \pi^-}|} = 2.59(1.34). \quad (24)$$

• D-wave mass and hadronic couplings

In the energy region where we shall work below 1.09 GeV, the D -wave contribution can be also important. However, an accurate parametrization of the D -wave contribution is not available. Assuming that it is dominated by the $f_2(1270)$, we extract its complex pole position and hadronic couplings and the corresponding “bare parameters” of the model from the fit of the $I = 0, J = 2$ phase shift measured in [24] and [25]. In so doing, we parametrize, as in [4], the $I = 0$ D -wave $\pi\pi \rightarrow \pi\pi/K\bar{K}$ scattering amplitudes:

$$T_{\pi K}^{J=2} = g_{\pi} g_K \left(\frac{s - 4m_\pi^2}{s - s_0} \right) \left(\frac{s - 4m_K^2}{s - s_0} \right) \mathcal{D}_{J=2}^{-1}, \quad (25)$$

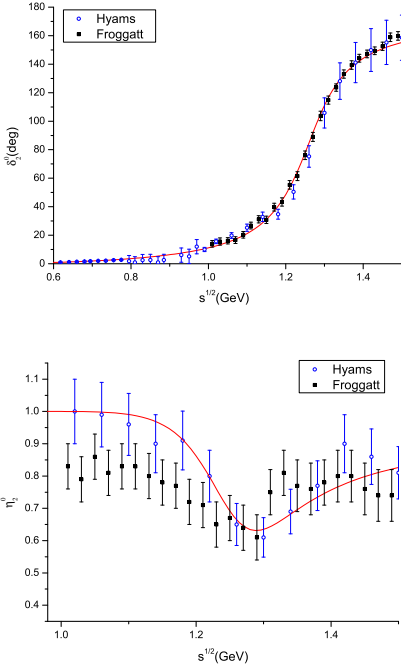


Figure 1: a) $I = 0$ D wave $\pi\pi$ phase; b) inelasticity. Experimental data are taken from [24, 25].

where s_0 is a pole on the negative real axis to simulate left hand singularity, and:

$$\mathcal{D}_{J=2}(s) = s_R - s - \sum_{P=\pi, K} g_P^2 C(s, m_P). \quad (26)$$

The function $C(s, m_P)$ satisfies:

$$\text{Im}C(s, m_P) = \rho_P(s) \left(\frac{s - 4m_P^2}{s - s_0} \right)^2, \quad (27)$$

with $\rho_P(s) = \sqrt{1 - 4m_P^2/s}$ the phase-space function. The real part of $C(s, m_P)$ can be obtained from dispersion relation:

$$\begin{aligned} C(s, m_P) &= \frac{2}{\pi} \left[\left(\frac{s - 4m_P^2}{s - s_0} \right)^2 \left(\frac{s - 4m_P^2}{m_P^2} \tilde{L}_1(s) + 1 \right) \right. \\ &\quad \left. - \frac{s(2s_0 - s)}{(s - s_0)^2} A - \frac{s}{s - s_0} B \right], \end{aligned} \quad (28)$$

where the last poles are adjusted to cancel the poles at $s = s_0$ and⁷:

$$\begin{aligned} A &= \left(\frac{s_0 - 4m_P^2}{s_0} \right)^2 \left[\frac{s_0 - 4m_P^2}{m_P^2} \tilde{L}_1(s_0) + 1 \right], \\ B &= \left(\frac{s_0 - 4m_P^2}{s_0} \right)^2 \left[2 \frac{s_0 + m_P^2}{m_P^2} \tilde{L}_1(s_0) + \frac{s_0 + 4m_P^2}{s_0 - 4m_P^2} + \frac{1}{2} \right]. \end{aligned} \quad (29)$$

⁷Note the extra factor 1/2 in B compared to the one in [4].

The resulting values of the bare parameters are given in Table 1, from which we derive the pole position in the 2nd sheet and the residues of $f_2(1270)$ ⁸. Compared with the PDG data⁹:

$$M_{f_2} = 1.27 \text{ GeV} \quad \text{and} \quad \Gamma_{f_2 \rightarrow \pi\pi} = 156.9^{+3.8}_{-1.2} \text{ MeV}, \quad (30)$$

one can notice that the pole position and the $\pi\pi$ width are well reproduced.

Table 1: Values in GeV^d ($d = 1, 2$) of the bare and physical parameters of the D -wave

$s_r = 2.06$	$s_0 = -1.25$	$g_\pi = 0.96$	$g_K = 1.38$
$M_{f_2} = 1.27 - i0.07$	$g_{f_2\pi\pi} = 0.48 - i0.03$	$g_{f_2\bar{K}K} = 0.28 - i0.06$	

• The vector meson contributions

In the energy-region where we shall work, exchange of vector mesons $V \equiv \rho, \omega, K^{*+}, K^{*0}$ in the t-channel can become important. We introduce their couplings to $\gamma\gamma$ via the effective interaction:

$$\mathcal{L}_{V\pi\gamma} = \frac{e}{4} \epsilon^{\mu\nu\rho\sigma} \sum_V h_V \pi V_{\mu\nu} F_{\rho\sigma}, \quad (31)$$

where $V_{\mu\nu} = \partial_\mu V_\nu - \partial_\nu V_\mu$ (resp. $F_{\mu\nu} = \partial_\mu F_\nu - \partial_\nu F_\mu$) are the vector (resp. electromagnetic) field strengths; π is the pion field. The coupling h_V is normalized as:

$$\Gamma(V \rightarrow \pi\gamma) = \frac{\alpha}{24} h_V^2 M_V^3 \left(1 - \frac{m_\pi^2}{M_V^2} \right)^3. \quad (32)$$

Using the standard vector form of the vector propagator, the Born contribution to the $\gamma\gamma \rightarrow \pi^+\pi^-$ amplitude due to the vector meson exchange is:

$$\begin{aligned} T_V^B &= \frac{\alpha h_V^2}{16} \left[\frac{(\epsilon_1 \cdot \epsilon_2)[t(s - u) + m_\pi^4] - 2s(\epsilon_1 \cdot p_1)(\epsilon_2 \cdot p_1)}{t - M_V^2} + \right. \\ &\quad \left. \frac{(\epsilon_1 \cdot \epsilon_2)[u(s - t) + m_\pi^4] - 2s(\epsilon_1 \cdot p_1)(\epsilon_2 \cdot p_1)}{u - M_V^2} \right], \end{aligned} \quad (33)$$

from which we deduce the helicity amplitudes:

$$\begin{aligned} F_V^B &= \frac{\alpha h_V^2}{16} \left[\frac{ts}{t - M_V^2} + \frac{us}{u - M_V^2} \right], \\ G_V^B &= \frac{\alpha h_V^2}{16} \left[\frac{t^2 + ts - 2m_\pi^2 t + m_\pi^4}{t - M_V^2} \right. \\ &\quad \left. + \frac{u^2 + us - 2m_\pi^2 u + m_\pi^4}{u - M_V^2} \right]. \end{aligned} \quad (34)$$

The results agree with the ones in the different literature (see e.g. [4, 26, 27]).

⁸There is also pole $(1.244 - i0.095)$ GeV in the 3rd sheet.

⁹Notice that the data of the inelasticity are not quite good which induces a relatively bad $\chi^2/ndf = 132.6/95 = 1.4$.

• The $B(1^{+-})$ axial-vector contributions

Their contributions can be introduced via the lowest order effective coupling [26]:

$$\mathcal{L}_{B\pi\gamma} = 3eh_B F_{\mu\nu} Tr(\bar{B}^\mu(Q, \partial^\nu\pi)) , \quad (35)$$

with:

$$\bar{B}_\mu = \begin{pmatrix} \frac{b_1^0}{\sqrt{2}} + \frac{h_1(1170)}{\sqrt{2}} & b_1^+(1235) \\ b_1^-(1235) & -\frac{b_1^0}{\sqrt{2}} + \frac{h_1(1170)}{\sqrt{2}} \end{pmatrix}_\mu , \quad (36)$$

and h_B is normalized as in Eq. (32). One can deduce the amplitude:

$$T_B^B = \frac{\alpha h_B^2}{16} \left[\frac{(\epsilon_1 \cdot \epsilon_2)(t - m_\pi^2)^2 - 2s(\epsilon_1 \cdot p_1)(\epsilon_2 \cdot p_1)}{t - M_B^2} \right. \\ \left. + \frac{(\epsilon_1 \cdot \epsilon_2)(u - m_\pi^2)^2 - 2s(\epsilon_1 \cdot p_1)(\epsilon_2 \cdot p_1)}{u - M_B^2} \right] , \quad (37)$$

Then, the helicity amplitudes are:

$$F_{b_1}^B = -\frac{\alpha h_{b_1}^2}{16} \left[\frac{ts}{t - M_{b_1}^2} + \frac{us}{u - M_{b_1}^2} \right] , \\ G_{b_1}^B = \frac{\alpha h_{b_1}^2}{16} \left[\frac{t^2 + ts - 2m_\pi^2 t + m_\pi^4}{t - M_{b_1}^2} \right. \\ \left. + \frac{u^2 + us - 2m_\pi^2 u + m_\pi^4}{u - M_{b_1}^2} \right] . \quad (38)$$

• The $a_1(1^{++})$ axial-vector contribution

We describe the $a_1(1^{++})$ in the same way as the $b_1(1^{+-})$ meson¹⁰, where h_{b_1} is simply replaced by h_{a_1} , which can either be determined from the $a_1 \rightarrow \pi\gamma$ width or from the ChPT coupling constants [27, 28]:

$$h_{a_1}^2 = \frac{4(L_9 + L_{10})}{f_\pi^2} = 0.656 \text{ GeV}^{-2} , \quad (39)$$

where $f_\pi = 92.4$ MeV is the pion decay constant.

• The size of the different radiative couplings

These can be extracted from the data and using $SU(3)$ symmetry relations and read in units of GeV^{-1} :

$$h_\rho = 0.82, \quad h_\omega = 2.39, \quad h_{K^{*+}} = 0.83, \quad h_{K^{*0}} = 1.27, \\ h_{a_1} = 0.81, \quad h_{b_1} = 0.65, \quad h_{h_1} = 3h_{b_1} . \quad (40)$$

5. K-matrix model analysis of $\gamma\gamma \rightarrow \pi\pi$ below 1.09 GeV

¹⁰A tensor formulation of the axial-vector meson has been proposed in [28] where the form of the propagator differs from the standard one. If we use this propagator, we reproduce the expression of the amplitude given in [27] where an extra contact term $s(\epsilon_1 \cdot \epsilon_2)$ is added in Eq. (37). We shall see in our analysis that the presence of this term would decrease the strength of the direct coupling of the scalar resonance but the total = direct+rescattering contribution remains almost unchanged. This term might be absorbed by some other counter terms of the complete effective lagrangian.

• The Born and unitarized S -wave amplitudes

The Born and unitarized terms can be calculated unambiguously using the effective lagrangians. Taking into account the t-channel exchange of pion, vector and axial-vector mesons discussed in the previous section and shown in Fig. 2, the Born and unitarized parts of the amplitude given in Eq. (16) generalize to (normalized to α):

$$\begin{pmatrix} T_\pi^u \\ T_K^u \end{pmatrix} = b_\pi \left(\begin{array}{cc} f_\pi^B + & \tilde{f}_\pi^B \tilde{T}_{\pi\pi} \\ \tilde{f}_\pi^B \tilde{T}_{\pi K} & \end{array} \right) + b_K \left(\begin{array}{cc} f_K^B + & \tilde{f}_K^B \tilde{T}_{K\pi} \\ \tilde{f}_K^B \tilde{T}_{KK} & \end{array} \right) \\ + \sum_{V=\rho,\omega} b_V h_V^2 \left(\begin{array}{cc} f_V^{BG} + & \tilde{f}_V^B \tilde{T}_{\pi\pi} \\ \tilde{f}_V^B \tilde{T}_{\pi K} & \end{array} \right) \\ + \sum_{V=K^{*+},K^{*0}} b_V h_V^2 \left(\begin{array}{cc} f_V^{BG} + & \tilde{f}_V^B \tilde{T}_{K\pi} \\ \tilde{f}_V^B \tilde{T}_{KK} & \end{array} \right) \\ + \sum_{A=a_1,b_1,h_1} b_A h_A^2 \left(\begin{array}{cc} f_A^{BG} + & \tilde{f}_A^B(A) \tilde{T}_{\pi\pi} \\ \tilde{f}_A^B \tilde{T}_{\pi K} & \end{array} \right) , \quad (41)$$

where the values of $h_{V,A}$ are in Eq. (40), $b_{\pi,\rho,\dots}$ are Clebsch-Gordan coefficients for projecting π, ρ, \dots exchanges on the $I = 0$ s-channel amplitudes:

$$\begin{aligned} b_\pi &= \sqrt{2}/\sqrt{3}, & b_\rho &= \sqrt{3}/\sqrt{2}, & b_\omega &= 1/\sqrt{6}, \\ b_K &= 1/\sqrt{2}, & b_{K^{*+}} &= b_{K^{*0}} = 1/\sqrt{2}, \\ b_{a_1} &= \sqrt{2}/\sqrt{3}, & b_{b_1} &= \sqrt{3}/\sqrt{2}, & b_{h_1} &= 1/\sqrt{6} . \end{aligned} \quad (42)$$

The partial S -wave Born amplitudes read :

$$\begin{aligned} f_P^B &= 2L_1 : P \equiv \pi, K ; \quad f_V^{BG} = \frac{s}{8}[1 - L_2] , \\ f_{a_1}^{BG} &= \frac{s}{8}[-1 + L_2] ; \quad f_{b_1}^{BG} = \frac{s}{8}[-1 + L_2] , \end{aligned} \quad (43)$$

where $L_1(s, m_P^2)$ and $L_2(s, m_\pi, M_{V,A}^2)$ are functions analytic in the left hand cut plane whose expressions are given in Appendix C of [4]. The reduced amplitudes are defined from the amplitudes in [1, 3] as:

$$\begin{aligned} \tilde{T}_{\pi\pi} &\equiv \frac{G}{\mathcal{D}_P} \equiv \frac{T_{\pi\pi}}{f_{\pi\pi}^2} = g_{\pi a}^2 P_{aa} + 2g_{\pi a} g_{\pi b} P_{ab} + g_{\pi b}^2 P_{bb} , \\ \tilde{T}_{K\pi} &= g_{\pi a} g_{K a} P_{aa} + (g_{\pi a} g_{K b} + g_{K a} g_{\pi b}) P_{ab} + g_{\pi b} g_{K b} P_{bb} \\ &= \tilde{T}_{\pi K} , \end{aligned} \quad (44)$$

where $f_{\pi a}$ is the shape function assumed to be the same for π and K . \tilde{f}_P^B ($P \equiv \pi, K$) is defined in Eq. (16) like \tilde{f}_P in Eq. (7) expressed in terms of the functions $h_P(s) - h_P(0)$ but with \tilde{L}_1 replaced by $-\tilde{L}_1$ everywhere. For vector meson exchanges, the triangle loop function is generalized to:

$$\tilde{f}_V^B(s) = \frac{1}{8\pi} [h_V^B(s) - h_V^B(0)] \quad (45)$$

where

$$\begin{aligned} h_V^B(s) &= f_P(s) \left[2M_V^2 \tilde{L}_2(s) - \frac{2s(s - 4m_P^2)}{m_P^2} \tilde{L}_1(s) \right. \\ &\quad \left. + s \left[\frac{2m_P^2 - M_V^2}{M_V^2} - \left(\frac{M_V^2}{M_V^2 - m_P^2} \right)^2 \ln \frac{M_V^2}{m_P^2} \right] \right] \end{aligned}$$

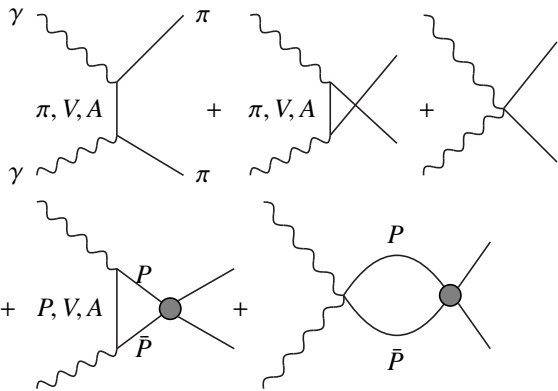


Figure 2: Born and Unitarized amplitudes T_P^u : $P \equiv \pi, K$; $V \equiv \rho, \omega$; $A \equiv b_1, h_1, a_1$.

$$\begin{aligned}
 & -\frac{\sigma_{N0}}{s - \sigma_D} \left[2M_V^2 \tilde{L}_2(\sigma_D) \right. \\
 & -\frac{2\sigma_D(\sigma_D - 4m_P^2)}{m_P^2} \tilde{L}_1(\sigma_D) \\
 & \left. + \sigma_D \left[\frac{2m_P^2 - M_V^2}{M_V^2} - \left(\frac{M_V^2}{M_V^2 - m_P^2} \right)^2 \ln \frac{M_V^2}{m_P^2} \right] \right], \quad (46)
 \end{aligned}$$

and where the functions $\tilde{L}_1(s)$ and $\tilde{L}_2(s)$ have been defined in the appendix C of [4].

For the axial-vector mesons, $h_A^B(s)$ is opposite in sign with the one for vector mesons given above.

• The Born and unitarized D -wave amplitudes

Here we shall discuss two models, namely the one originally discussed in [4] and a new model with a shape function inspired from the S -wave channel and which is expected to have a much better analytic property (absence of a pole in the left cut). We shall assume that the D -wave contribution is dominated by the helicity two $I = 0$ amplitude which will be verified (a posteriori) from a fit analysis.

– *The original model* has been discussed in details in [4]. For one pion exchange, the isospin $I = 0$ $\gamma\gamma \rightarrow \pi\pi$ amplitude is:

$$T_\pi^u = \sqrt{\frac{2}{3}} \left[f_\pi^B + g_\pi^2 \tilde{f}_\pi^B \left(\frac{s - 4m_\pi^2}{s - s_0} \right) \mathcal{D}_{J=2}^{-1} \right] \quad (47)$$

where f_π^B is the Born term with helicity 2:

$$f_\pi^B = \frac{3}{8} \left[\frac{1}{3} - \frac{2m_\pi^2}{s - 4m_\pi^2} + \frac{8m_\pi^2}{s - 4m_\pi^2} L_1(s) \right], \quad (48)$$

and the unitary triangle one loop function \tilde{f}_π^B satisfies:

$$\text{Im} \tilde{f}_\pi^B = \theta(s - 4m_P^2) \rho_P f_P^B \frac{s - 4m_P^2}{s - s_0}. \quad (49)$$

The real part of \tilde{f}_π^B can be derived from dispersion relation with subtraction at $s = 0$:

$$\tilde{f}_\pi^B = \frac{3}{4} \left[-\frac{s - 4m_\pi^2}{s - s_0} \left(2 - \frac{s - 4m_\pi^2}{3m_\pi^2} \right) \tilde{L}_1 - 4 \frac{s - 4m_\pi^2}{s - s_0} \tilde{L}_1^2 \right]$$

$$+ \frac{A_2 m_\pi^2}{s - s_0} + B_2 \right], \quad (50)$$

where

$$\begin{aligned}
 A_2 &= \frac{s_0 - 4m_\pi^2}{m_\pi^2} \tilde{L}_1(s_0) \left[\left(2 - \frac{s_0 - 4m_\pi^2}{3m_\pi^2} \right) + 4\tilde{L}_1(s_0) \right], \\
 B_2 &= \frac{m_\pi^2}{s_0} \left(\frac{13}{3} + A_2 \right).
 \end{aligned} \quad (51)$$

– *The new model* is introduced to avoid the left hand pole at $s = s_0$ of the old model. In this case the amplitude reads:

$$T_\pi^u = \sqrt{\frac{2}{3}} \left[f_\pi^B + g_\pi^2 \tilde{f}_\pi^B|_{\text{new}}(s - 4m_\pi^2) \mathcal{D}_{J=2}^{-1} \right], \quad (52)$$

where the 2nd term is the unitarized amplitude. $\tilde{f}_\pi^B|_{\text{new}}$ is the triangle loop function due to one pion exchange:

$$\text{Im} \tilde{f}_\pi^B|_{\text{new}} = \theta(s - 4m_P^2) \rho_P f_P^B \frac{s - 4m_P^2}{(s - s_0)^2}. \quad (53)$$

The real part of $\tilde{f}_\pi^B|_{\text{new}}$ can be derived from dispersion relation with subtraction at $s = 0$:

$$\begin{aligned}
 \tilde{f}_\pi^B|_{\text{new}} &= \frac{3}{4} \left[-\frac{s - 4m_\pi^2}{(s - s_0)^2} \left(2 - \frac{s - 4m_\pi^2}{3m_\pi^2} \right) \tilde{L}_1 \right. \\
 &- 4 \frac{s - 4m_\pi^2}{(s - s_0)^2} \tilde{L}_1^2 + \frac{A_2 m_\pi^2}{(s - s_0)^2} + \frac{B'_2}{s - s_0} \\
 &\left. - \left(\frac{13}{3} \frac{m_\pi^2}{s_0^2} + \frac{A_2}{s_0^2} + \frac{B'_2}{-s_0} \right) \right], \quad (54)
 \end{aligned}$$

with:

$$B'_2 = \lim_{s \rightarrow s_0} \frac{d}{ds} \left[(s - 4m_\pi^2) \left(2 - \frac{s - 4m_\pi^2}{3m_\pi^2} \right) \tilde{L}_1 - 4(s - 4m_\pi^2) \tilde{L}_1^2 \right] \quad (55)$$

We compare these two models in Fig. 3, where we can notice that the two models lead (almost) to the same amplitudes. From this figure, it is interesting to notice that there is a strong cancellation between the Born term and the real part of the unitarized amplitude around the $f_2(1270)$ pole, while the imaginary part of the amplitude is relatively small. This feature demonstrates that the $\gamma\gamma$ total width of the f_2 is dominated by its direct coupling as expected. In the following, we shall use the old model for our fitting procedure due only to a chronological procedure of our analysis.

• The direct resonance couplings

On the contrary the direct couplings of the resonances are model dependent where the polynomial \mathcal{P} reflects the ambiguity from the dispersion relations¹¹. We parametrize this contribution by introducing the effective photon-photon-resonance couplings for the S -waves [4]:

$$T_\pi^S \equiv \alpha \frac{\mathcal{P}}{\mathcal{D}_P} = \alpha \frac{\sqrt{2}s}{\mathcal{D}_P} \left[(f_{\sigma\gamma} + s f'_{\sigma\gamma}) \tilde{T}_{\sigma\pi} + (f_{f_0\gamma} + s f'_{f_0\gamma}) \tilde{T}_{f_0\pi} \right], \quad (56)$$

¹¹In [29] these polynomial (subtraction constants) are related to the pion polarizabilities.

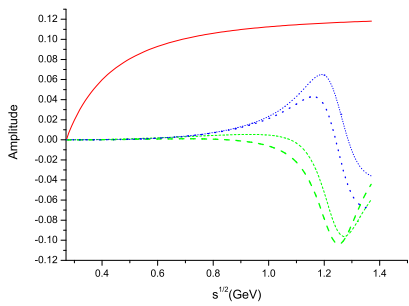


Figure 3: D-wave amplitudes in the two different models. Born term (continuous - red line). Original model [4]: real part (dashed line - green); imaginary part (dotted line - blue). New model: the same as for the original model but with thick lines.

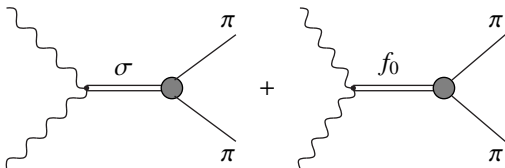


Figure 4: Direct couplings of the resonances to $\gamma\gamma$

where the reduced amplitudes are:

$$\begin{aligned}\tilde{T}_{\pi\sigma} &= [g_{\pi a}(s_{Rb} - s) - g_{Kb}(g_{\pi a}g_{Kb} - g_{Ka}g_{\pi b})\tilde{f}_K], \\ \tilde{T}_{\pi f_0} &= [g_{\pi b}(s_{Ra} - s) - g_{Ka}(g_{\pi b}g_{Ka} - g_{Kb}g_{\pi a})\tilde{f}_K].\end{aligned}\quad (57)$$

The functions $f_0(s)$, $\tilde{f}_P(s)$ ($P = \pi, K$), $\mathcal{D}_P(s)$ and bare parameters σ_D , s_A , s_{Ra} , $g_{\pi a}$, g_{Ka} , s_{Rb} , $g_{\pi b}$, g_{Kb} are defined in [1, 3] and given in Tables 2 and 3 of ref. [3]. Similarly, we have for the D -waves [4]:

$$T_\pi^D = \left(\frac{\alpha}{\sqrt{2}}\right) \left[s^2 f_{f_2\gamma}^{l=0} + s f_{f_2\gamma}^{l=2} \right] \tilde{T}_{\pi f_2}, \quad (58)$$

with the normalization:

$$\Gamma_{f_2 \rightarrow \gamma\gamma} = \frac{4}{3} \left(\alpha f_{2\gamma}^{l=2} \right)^2 M_{f_2}^3, \quad (59)$$

if one assumes that the $\lambda = 0$ helicity contribution is negligible¹². Using the PDG value (2.6 ± 0.24) keV [23] for the $\gamma\gamma$ width, we deduce:

$$|f_{2\gamma}^{l=2}| = 0.136 \text{ GeV}^{-1}. \quad (60)$$

¹²If we let free the two couplings of the $\lambda = 0$ and 2 components of the $f_2(1270)$ in the fit, we find that the $\lambda = 0$ coupling is negligible confirming our assumption. We also notice that at the f_2 -pole, there is a strong cancellation between the Born and rescattering contributions (see also [4]) which justifies the identification of the $f_2 \rightarrow \gamma\gamma$ total width given by PDG [23] to the “direct” width.

6. Fitting $\gamma\gamma \rightarrow \pi^0\pi^0$ just above the $\bar{K}K$ threshold

• Fitting procedure

In so doing, we fix the value of the $\lambda = 2$ components of the $f_2(1270)$ using the $f_2 \gamma\gamma$ width given by PDG and neglect the $\lambda = 0$ one. We use as inputs the Set 2 and Set 3 hadronic parameters obtained in [3] using the largest range of hadronic data. Then, we perform a fit of the four direct couplings from the total and differential cross-sections until a value of $\sqrt{s} \approx 1$ GeV¹³. We move \sqrt{s} around 1 GeV and look for the minimum χ^2/ndf for the total cross-section, which is obtained at $\sqrt{s} = 1.09$ GeV, where $\chi^2/ndf = 39.5/41 = 0.96$ for e.g. Set 3 of the hadronic parameters, which we show in Fig. 5. The results of the fit are

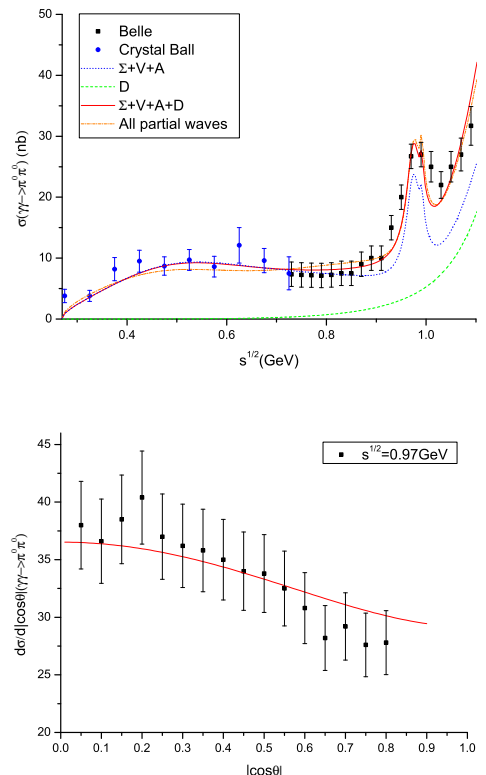


Figure 5: Fit of the $\gamma\gamma \rightarrow \pi^0\pi^0$ total ($\sqrt{s} \leq 1.09$ GeV and $|\cos \theta| \leq 0.8$) and differential ($\sqrt{s} \leq 0.97$ GeV) cross-sections for the Set 3 of hadronic parameters [3], where $\chi^2/ndf = 39.5/41 = 0.96$ is minimal. The data come from Crystal Ball (blue full circle) and from Belle (black full square); dotted blue (S-channel contribution); dashed green (D-wave contribution); continuous red (total contribution).

given in Tables 2 and 3.

• Comments on the results

Our results are summarized in Tables 3 and 4:

– *The direct part of the $\gamma\gamma$ widths:* one can notice that the K exchange and K -loop tend to decrease the direct width of the σ meson which is compensated by the V+A contributions, such that at the end, the final result is compatible with the one 0.13

¹³We prevent to fit until 1.4 GeV in order to avoid the possible contribution of an eventual $f_0(1370)$ and to minimize the contribution of the D -wave.

Table 2: Fitted values of the bare couplings of σ and $f_0(980)$ in units of GeV^{-1} for $(f_{\sigma\gamma})$ and GeV^{-2} for $(f'_{\sigma\gamma})$ using Set 2 and Set 3 of the hadronic parameters from [3]. The $\gamma\gamma \rightarrow \pi\pi$ total cross-section has been fitted until $\sqrt{s}=1.09$ GeV (minimum value of χ^2/ndf) and the differential cross-section until $\sqrt{s}=0.97$ GeV.

	$f_{\sigma\gamma}$	$f'_{\sigma\gamma}$	$f_{f_0\gamma}$	$f'_{f_0\gamma}$	χ^2/ndf
Set 2	2.68	-2.70	0.85	-1.18	51.4/41=1.25
Set 3	3.03	-3.07	1.03	-1.43	39.5/41=0.96

keV obtained in the case: 1 resonance \oplus 1 channel obtained below 0.7 GeV [1]. We consider as a final result the average from Set 2, Set 3 and from the one resonance \oplus one channel analysis below 0.7 GeV of [1] for the σ and the average from Set 2 and Set 3 for the $f_0(980)$ (see Table 4):

$$\Gamma_{\sigma}^{dir} = 0.16(4) \text{ keV}, \quad \Gamma_{f_0}^{dir} \simeq 0.28(1) \text{ keV}. \quad (61)$$

For a consistent comparison with some other theoretical estimates (QSSR,...) obtained in the real axis, we translate these widths from the residues to the one evaluated at the on-shell σ mass or Breit-Wigner mass defined in [1, 30] when the amplitude is purely imaginary at the phase 90° :

$$\text{Re } \mathcal{D}(M_{\sigma}^2) = 0 \implies M_{\sigma}^{os} \simeq 0.92 \text{ GeV}. \quad (62)$$

In this way, we obtain:

$$\Gamma_{\sigma}^{dir}|_{on-shell} = 1.2(3) \text{ keV}, \quad \Gamma_{f_0}^{dir}|_{on-shell} \approx \Gamma_{f_0}^{dir}, \quad (63)$$

which are similar with the results obtained by using a Breit-Wigner parametrization of the data [1].

– The rescattering part of the $\gamma\gamma$ widths are (in units of keV):

$$\Gamma_{\sigma}^{resc} = 1.89(81) \text{ keV}, \quad \Gamma_{f_0}^{resc} = 0.85(5) \text{ keV}, \quad (64)$$

where we take the average from Set 2, Set 3 and from the one resonance \oplus one channel analysis below 0.7 GeV of [1] for the σ and the average from Set 2 and Set 3 for the $f_0(980)$ (see Table 4). One can notice that in both cases, the rescatterings are relatively large indicating the important rôle of meson loop contributions in the $\gamma\gamma$ widths of the scalar mesons. The large couplings of scalar to meson loops are often interpreted in the current literature as being related to their four-quark or/and molecule structure. However, these large couplings to $\pi\pi$ and $\bar{K}K$ are also expected if the σ , f_0 have large gluon component and violate OZI rule in their hadronic decays [10, 12, 13]. In the case of the σ meson, one can notice the large effect due to vector mesons which is partly compensated by the one of the axial-vector mesons. Compared with the result 2.7 keV from the analysis below 0.7 GeV with a pion loop [1], one can notice that Γ_{σ}^{resc} has been affected by the presence of the $f_0(980)$ when doing the fitting procedure. In the case of the $f_0(980)$, the effect of the K and of $V + A$ are quite important

– The total \equiv direct + rescattering part of the $\gamma\gamma$ widths are (in units of keV):

$$\Gamma_{\sigma}^{tot} = 3.08(82) \text{ keV}, \quad \Gamma_{f_0}^{tot} = 0.16(1) \text{ keV}. \quad (65)$$

Table 3: The same fitting procedure as in Table 2 but for the physical couplings (in units of $\alpha \times 10^{-3}$ GeV) and for the two photon widths (in units of keV) of the σ and $f_0(980)$. Each contributions of different mesons exchanged in the t-channel and in the loops are shown explicitly. D corresponds to the D -wave contribution.

Fit	π	$\Sigma \equiv \pi+K$	$\Sigma+V$	$\Sigma+A$	$\Sigma+V+A$	$\Sigma+D$	$\Sigma+V+A+D$
Set 2							
g_{σ}^{dir}	-2+49i	19+15i	26+19i	10+22i	20+27i	8+24i	9+37i
g_{σ}^{resc}	65+99i	66+103i	-23+185i	131+28i	42+109i	66+103i	42+109i
g_{σ}^{tot}	63+148i	85+118i	3+204i	141+50i	62+136i	74+127i	51+146i
Γ_{σ}^{dir}	0.27	0.06	0.11	0.07	0.13	0.07	0.16
Γ_{σ}^{resc}	1.60	1.71	3.97	2.05	1.53	1.71	1.53
Γ_{σ}^{tot}	2.90	2.36	4.66	2.51	2.50	2.43	2.67
$g_{f_0}^{dir}$	-125+3i	-4-5i	-109-18i	26-6i	-75-14i	-5-4i	-73-12i
$g_{f_0}^{resc}$	12+12i	95+16i	47+16i	178+14i	130+14i	95+16i	131+14i
$g_{f_0}^{tot}$	-113+15i	91+11i	-62-2i	204+8i	55	90+12i	52+2i
$\Gamma_{f_0}^{dir}$	0.82	0.002	0.63	0.04	0.31	0.002	0.29
$\Gamma_{f_0}^{resc}$	0.02	0.48	0.13	1.67	0.90	0.48	0.90
$\Gamma_{f_0}^{tot}$	0.68	0.43	0.20	2.19	0.16	0.42	0.17
Set 3							
g_{σ}^{dir}	18+29i	12+28i	27+16i	0.2+42i	17+33i	0.3+36i	5+42i
g_{σ}^{resc}	58+96i	58+100i	-41+191i	132+20i	33+109i	58+100i	33+109i
g_{σ}^{tot}	76+125i	70+128i	-14+207i	132+62i	50+142i	58+136i	37+152i
Γ_{σ}^{dir}	0.13	0.10	0.11	0.19	0.15	0.14	0.20
Γ_{σ}^{resc}	1.36	1.44	4.22	1.94	1.43	1.44	1.43
Γ_{σ}^{tot}	2.34	2.35	4.70	2.32	2.49	2.43	2.67
$g_{f_0}^{dir}$	-99+42i	-10-8i	-95-14i	22-8i	-65-11i	-13-7i	-71-10i
$g_{f_0}^{resc}$	12+8i	96+6i	51+7i	170+3i	124+4i	96+6i	124+15i
$g_{f_0}^{tot}$	-87+50i	86-2i	-44-7i	192-5i	59-7i	83-i	54+5i
$\Gamma_{f_0}^{dir}$	0.61	0.01	0.48	0.03	0.23	0.01	0.27
$\Gamma_{f_0}^{resc}$	0.01	0.49	0.14	1.51	0.81	0.49	0.81
$\Gamma_{f_0}^{tot}$	0.53	0.39	0.10	1.93	0.19	0.36	0.15

7. Comparison with some other results

• Dispersion relations

A comparison of the total width in Eq. (65) with the results obtained using dispersion relations [8, 27, 31, 32]¹⁴ is shown in Table 4 can only be done for the total width because a separation of the direct and rescattering processes have not been done in this approach. Our results for the σ are in better agreement with the ones from [1, 8, 31]. The one of the f_0 is in between the results of [8, 31] and of the PDG value [23]. However, the PDG value seems to be more consistent with our value of the direct width which might be identified with the one using a Breit-Wigner parametrization of the data.

• Model of [34]

This approach of [9, 34, 35] presents some similarities with ours where the direct and rescattering processes can be also sep-

¹⁴Some calculations based on the π and K loops can also be found in [33].

Table 4: Summary of the fitted values of the $\gamma\gamma$ decay width (in unit of keV) using Set 2 and Set 3 of hadronic parameters from [3] and comparison with some other determinations and the PDG08 value. The total cross-section has been fitted until $\sqrt{s} = 1.09$ GeV (minimum value of χ^2/ndf) and the differential cross-section until $\sqrt{s} = 0.97$ GeV. The best $\chi^2/ndf = 0.96$ is obtained from Set 3.

	Set 2	Set 3	[1]	[27]	[31]	[31]	[8]	[32]	[34]	PDG [23]
\sqrt{s}	1.09	1.09	0.8	0.8	1.44	1.44	1.4		1.44	
$r_{0/2}$	0.0	0.0			0.13	0.26	0.15			
Γ_{σ}^{dir}	0.16	0.20	0.13				0.010			
Γ_{σ}^{resc}	1.53	1.43	2.70							
Γ_{σ}^{tot}	2.67	2.67	3.90	1.7	3.1	2.4	2.1	1.2		
$\Gamma_{f_0}^{dir}$	0.29	0.27					0.015			
$\Gamma_{f_0}^{resc}$	0.90	0.81								
$\Gamma_{f_0}^{tot}$	0.17	0.15		0.42	0.10	0.13			0.29 ± 0.08	

arated. However, we differ on the treatment of the hadronic $\pi\pi \rightarrow \pi\pi/\bar{K}K$ process as a background phase has been explicitly introduced in addition to the resonance contributions in [9, 34, 35]. Besides this difference, we look in details into the analysis of [34]:

– We notice that the authors use the bare couplings for predicting the $\gamma\gamma$ width of the resonances while we transform the bare couplings (which are real numbers) to the residues in the complex plane by analytically continuing these results to the 2nd sheet. In fact, working with the bare couplings for the wide complex σ meson cannot (a priori) be a good approximation.

– We also notice that the authors only include the S and D -waves but discard the contributions due to the vector and axial-vector mesons (V+A) which are important in the analysis. However, though the numerical fits are similar (see Fig. 5) with a slightly larger $\chi^2/ndf = 1.16$ for $\Sigma + D$ -waves, instead of 0.96 for $\Sigma + D + V + A$, the values of the widths are largely affected as one can deduce from the last two columns of Table 3.

– If one uses the previous inputs (bare couplings + S and D -waves), one can see from the value of the bare coupling obtained in [1] that the direct width of the σ would be about 0.02 keV for a σ mass of 0.42 GeV, while the one of the $f_0(980)$ is about (0.002-0.01) keV from the column $\Sigma + D$ of Table 3. For the latter, we have assumed that the bare and physical couplings are about the same, which can be a good approximation because the $f_0(980)$ is narrow. These results agree with the ones of [34] but might not be realistic due the drawbacks which we have mentioned above.

• $\gamma\gamma \rightarrow \pi^+\pi^-/K^+K^-$ data

We use the previous fitted values of the parameters from $\gamma\gamma \rightarrow \pi^0\pi^0$ for predicting the $\gamma\gamma \rightarrow \pi^+\pi^-$ process. The result is shown in Fig. 6, where one can notice that the prediction is not good between 0.5 to 0.9 GeV if one only retains the S and D -waves in the partial waves of the Born term. A similar problem has been encountered by [34] (Fig 4) which they solve (Fig. 6) by introducing a form factor (which looks ad hoc) from [36] for the D -wave Born contribution which is important in the charged chan-

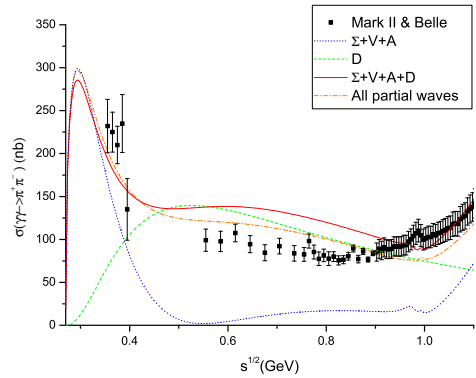


Figure 6: Predictions of the $\gamma\gamma \rightarrow \pi^+\pi^-$ total ($\sqrt{s} \leq 1.09$ GeV and $|\cos \theta| \leq 0.6$) using the fitted parameters from $\gamma\gamma \rightarrow \pi^0\pi^0$. The data come from Mark II and Belle: dotted blue (S-channel contribution including direct couplings); dashed green (D-wave contribution); continuous red (S+D partial waves); dot-dashed (sum of all partial waves)

nel¹⁵. Instead, we improve our analysis by adding all higher partial waves in the Born term and by including the direct terms of the S -waves. One can see in Fig. 6, that the predictions using the parameters from $\gamma\gamma \rightarrow \pi^0\pi^0$ are quite good compared with the data without introducing any ad hoc form factors.

8. On some possible substructures of the σ and $f_0(980)$

Our work has been motivated for shedding light on the possible substructure of the $\sigma/f_0(600)$ and $f_0(980)$ by analyzing their $\gamma\gamma$ widths, where the value of direct width is of special interest for a comparison with theoretical calculations based on quark and/or gluon loops.

– *The σ meson:* in our previous analysis of the hadronic couplings [2, 3] from $\pi\pi \rightarrow \pi\pi$, $\bar{K}K$ processes, we have noticed that because of the large size of its coupling to $\pi\pi$ and $\bar{K}K$ [$|g_{\sigma K^+K^-}|/|g_{\sigma\pi^+\pi^-}| = 0.37(6)$] (see also [4, 7, 8]), the σ cannot be mainly a $\pi\pi$ molecule or/and a four-quark state components, while its broad width cannot be explained by a large $\bar{q}q$ component. These observations go in line to a large gluon component expected from a low-energy theorem analysis in [10, 12, 13]¹⁶. The averaged result of the $\gamma\gamma$ direct width of about 1.2(3) keV (see Eq. 63), when runned at the on-shell σ mass, can indicate an eventual large gluon component of the σ ¹⁷. Moreover, our result seems to rule out a large four-quark component which has a too small direct $\gamma\gamma$ width of about some few eV [41] from QSSR or from some σ -like models [42].

¹⁵A similar observation can be done for the process $\gamma\gamma \rightarrow K^+K^-$, where the Born contributions due to the S and D -waves are also very important and dominates over the scalar meson contributions, as can be shown in Fig. 10 of [37], which we have checked.

¹⁶A large gluon component of the σ meson with a Breit-Wigner mass and width of about 1 GeV has been also advocated in [17]. A large gluon component for the σ and $f_0(980)$ also emerges from a calculation of the gluonium spectrum using a Nambu-Jona-Lasinio model [18].

¹⁷An isoscalar $S_2 \equiv (1/\sqrt{2})(\bar{u}u + \bar{d}d)$ state is expected to have a $\gamma\gamma$ width of about 4 keV [12, 13] from QCD spectral sum rules (QSSR) [38, 39] and quark model [40], while a pure gluonium state σ_B with $M_{\sigma_B} = 1$ GeV has a width of about (0.2-0.6) keV [10, 12] from some low-energy theorems.

– The $f_0(980)$: the direct $\gamma\gamma$ width of 0.27 keV for the $f_0(980)$ in Eq. (61) is neither compatible with a large four-quark component (too small) nor with a large S_2 component (too big). A pure $\bar{s}s$ component where a $\gamma\gamma$ width is expected to be about 0.4 keV [12, 13, 43] is not however favoured because of the non-zero coupling of $f_0(980)$ to $\pi\pi$ [$|g_{f_0 K^+ K^-}|/|g_{f_0 \pi^+ \pi^-}| = 2.59(1.34)$] obtained in [2, 3].

9. Gluonium production from J/ψ and ϕ radiative decays

The previous possible gluonium assignement of the σ and $f_0(980)$ can be tested from the J/ψ and ϕ radiative decays. This can be done following the work of [44], using dispersion relation techniques and the Euler-Heisenberg effective Lagrangian, where the gluonic part of the amplitude can be converted into the non-perturbative matrix element $\langle 0|\alpha_s G^2|S\rangle \sim M_S^2 f_S$, where the decay constant f_S ($S \equiv \sigma_B, G$) can be obtained from QSSR which predicts two scalar gluonia ($\sigma_B(1)$ coupled strongly to $\pi\pi, \bar{K}K$ due to OZI violations and the $G(1.5-1.6)$ coupled to $\eta'\eta', \eta\eta'$ obtained using quenched lattice) [10, 12, 13]. In this way, one obtains:

$$\begin{aligned} \Gamma(J/\psi \rightarrow S\gamma) &\simeq \frac{\alpha^3 \pi}{\beta_1^2 656100} \left(\frac{M_{J/\psi}}{M_c} \right)^4 \left(\frac{M_S}{M_c} \right)^4 \times \\ &\quad \frac{\left(1 - M_S^2/M_{J/\psi}^2 \right)^3}{\Gamma(J/\psi \rightarrow e^+ e^-)} f_S^2, \end{aligned} \quad (66)$$

where $\beta_1 = -1/2(11 - 2n_f/3)$ for $SU(n)_f$ is the first coefficient of the β function; M_c is the constituent charm quark mass which we take to be about $M_{J/\psi}/2$. Using the decay constant $f_S \equiv f_{\sigma_B} \simeq (1.4 \sim 1.0)$ GeV for $M_{\sigma_B} \simeq (0.75 - 1)$ GeV [10, 12, 13], one predicts:

$$B(J/\psi \rightarrow \sigma_B \gamma) \times B(\sigma_B \rightarrow \text{all}) \simeq (0.4 \sim 1.0) \times 10^{-3}, \quad (67)$$

which one can compare with [23]: $B(J/\psi \rightarrow \eta'\gamma) \simeq (4.7 \pm 0.27) \times 10^{-3}$ and $B(J/\psi \rightarrow f_2\gamma) \simeq (1.43 \pm 0.11) \times 10^{-3}$. Applying this result to the case of the $G(1.5-1.6)$ glueball of higher mass, one obtains [10, 12, 13]:

$$B(J/\psi \rightarrow G\gamma) \simeq (5.0 \pm 3.8) \times 10^{-4}, \quad (68)$$

where we have used $f_G \simeq (0.39 \pm 0.15)$ GeV. This prediction, which needs to be improved, is in agreement with the experimental lower bound of $(5.7 \pm 0.8) \times 10^{-4}$ [23]. Extrapolating this analysis to the case of the ϕ -meson, one obtains by using the strange quark constituent mass $M_s \simeq M_\phi/2$:

$$B(\phi \rightarrow S\gamma) \simeq 1.2 \times 10^{-4}, \quad (69)$$

which, despite the crude approximation used, compares quite well with the data [23]: $B(\phi \rightarrow \pi^+ \pi^- \gamma) \simeq (0.41 \pm 0.1) \times 10^{-4}$ and $B(\phi \rightarrow f_0(980)\gamma) \simeq (3.22 \pm 0.19) \times 10^{-4}$.

10. Gluonium production from D_s semi-leptonic decays

An analogous analysis has been done for D_s semileptonic decays, where one expects that the gluonium production will be of similar strength as the one for a $\bar{q}q$ state [45]:

$$\frac{\Gamma[D_s \rightarrow \sigma_B(gg)l\nu]}{\Gamma[D_s \rightarrow S_2(\bar{q}q)l\nu]} \approx \frac{1}{|f_+(0)|^2} \left(\frac{f_{\sigma_B}}{M_c} \right)^2 \simeq \mathcal{O}(1), \quad (70)$$

for $f_{\sigma_B} \approx 1$ GeV, where $|f_+(0)| \approx 0.5$ [46] is the form factor associated to the $\bar{q}q$ semileptonic production. Some other hadronic processes like $J/\psi \rightarrow \omega, \phi + \pi\pi/\bar{K}K$ (see e.g. [5]) and $D_{(s)}, B_{(s)} \rightarrow 3\pi, \dots$ (see e.g. [47]) decays can also be studied, but the mechanism for the decays are expected to be more complex than the one of radiative and semi-leptonic processes discussed previously. However, these analysis emphasize the important rôle of the kaon loops contributions, which in our approach are due to the rescattering contributions. We plan to come back to these issues in a future work.

11. Conclusions

At first sight, a $\bar{q}q$ -gluonium mixing scheme like the one proposed below 1 GeV in [12, 48] might be appropriate for describing the σ and $f_0(980)$ obtained from our fits of $\pi\pi \rightarrow \pi\pi/\bar{K}K$ and $\gamma\gamma \rightarrow \pi\pi$ scatterings. The values of their “direct widths” favour a large gluon content for the σ meson but are not decisive for explaining the substructure of the $f_0(980)$ meson. However, the large values of the rescattering widths, due to meson loops because of the large couplings of the σ and $f_0(980)$ to $\pi\pi$ or/and $\bar{K}K$, can be also obtained if they are gluonia states but not necessarily if they are four-quark (diquark-antidiquark) or molecule states as currently claimed in the existing literature. The agreement of our predictions for a gluonium production through radiative ϕ radiative decays with the data seems to support some large gluon component for the σ and to a lesser extent for the $f_0(980)$. This test can be pursued in the analysis of J/ψ radiative and D_s semi-leptonic decays. We plan to analyze in details the substructure of these light scalar mesons by including mixings in a future work.

Acknowledgements

We thank Eduardo de Rafael and Jose Oller for communications and discussions. We also thank Wolfgang Ochs for comments on the preliminary draft and for several email exchanges. This work has been partly supported by CNRS-IN2P3 within the project Non-perturbative QCD and Hadron Physics. X.G. Wang thanks the Laboratoire de Physique Théorique et Astroparticulaires (LPTA) of Montpellier for the hospitality.

References

- [1] G. Mennessier, S. Narison, W. Ochs, *Phys. Lett. B* **665** (2008) 205; *Nucl. Phys. Proc. Suppl.* **238** (2008) 181; G. Mennessier, P. Minkowski, S. Narison, W. Ochs, HEP MAD 07 Conference, SLAC Econf C0709107, *arXiv: 0707.4511 [hep-ph]* (2007).
- [2] R. Kaminski, G. Mennessier and S. Narison, *Phys. Lett. B* **680** (2009) 148.
- [3] G. Mennessier, S. Narison and X.-G. Wang, *Phys. Lett. B* **688** (2010) 59.
- [4] G. Mennessier, *Z. Phys. C* **16** (1983) 241; O. Babelon et al., *Nucl. Phys. B* **113** (1976) 445.
- [5] A. Pean, Thèse Montpellier (1992) (unpublished) and references therein.
- [6] J. Layssac, S. Narison, *Nucl. Phys. Proc. Suppl.* **186** (2009) 203.
- [7] R. Kaminski, L. Lesniak and B. Loiseau, *Phys. Lett. B* **413** (1997) 130; *Eur. Phys. J. C* **9** (1999) 141; D.V. Bugg, *Eur. Phys. J. C* **47** (2006) 45; M. Ablikim et al., *Phys. Lett. B* **607** (2005) 243.
- [8] Y. Mao, X.-G. Wang, O. Zhang, H.-Q. Zheng, Z.-Y. Zhou, *Phys. Rev. D* **79** (2009) 116008.
- [9] N.N. Achasov, A.V. Kiselev, *Phys. Rev. D* **73** (2006) 054029.
- [10] S. Narison, G. Veneziano, *Int. J. Mod. Phys. A* **4** (1989) 2751.

[11] V.A. Novikov et al., *Nucl. Phys.* **B 191** (1981) 301.

[12] S. Narison, *Nucl. Phys.* **B 509** (1998) 312; *Nucl. Phys. Proc. Suppl.* **64** (1998) 210; *Z. Phys. C* **26** (1984) 209; *Nucl. Phys. A* **675** (2000) 54c; *Nucl. Phys. Proc. Suppl.* **96** (2001) 244; *Nucl. Phys. A* **675** (2000) 54C; *Nucl. Phys. Proc. Suppl.* **121** (2003) 131.

[13] S. Narison, *Phys. Rev.* **D 73** (2006) 114024; *Nucl. Phys. Proc. Suppl.* **186** (2009) 306.

[14] J. Ellis and J. Lanik, *Phys. Lett.* **B 150** (1985) 289; *Phys. Lett.* **B 175** (1986) 83; J. Lanik, *Z. Phys. C* **39** (1988) 143.

[15] P. Di Vecchia and G. Veneziano, *Nucl. Phys.* **B 171** (1980) 253; P. Jain, R. Johnson and J. Schechter, *Phys. Rev.* **D 35** (1987) 2230.

[16] R.J. Crewther, *Phys. Rev. Lett.* **28** (1972) 1421; J. Ellis and M.S. Chanowitz, *Phys. Lett.* **B 40** (1972) 397; *Phys. Rev.* **D 7** (1973) 2490.

[17] P. Minkowski and W. Ochs, *Eur. Phys. J. C* **9** (1999) 283; *Nucl. Phys. Proc. Suppl.* **121** (2003) 119; *Eur. Phys. J. C* **39** (2005) 71; W. Ochs, *Nucl. Phys. Proc. Suppl.* **174** (2007) 146.

[18] M. Frasca, *arXiv: 1007.4479 [hep-ph]* (2010) and references therein.

[19] E. Ruiz Arriola and W. Broniowski, *Phys. Rev.* **D 81** (2010) 054009.

[20] K. Abe et al., BELLE collaboration, *arXiv: 0711.1926 [hep-ex]* (2007); T. Mori et al., *J. Phys. Soc. Jap.* **76** (2007) 074102.

[21] H. Marsiske et al., Crystal Ball collaboration, *Phys. Rev.* **D 41** (1990) 3324.

[22] J. Boyer et al., MARK II Collaboration, *Phys. Rev.* **D42** (1990) 1350.

[23] PDG 08, C. Amsler et al., *Phys. Lett.* **B 667** (2008) 1.

[24] C.D. Frogatt and J.L. Petersen, *Nucl. Phys.* **B 91** (1975) 454; **B 129** (1977) 89.

[25] B. Hyams et al., *Nucl. Phys.* **B 64** (1973) 134.

[26] J. Gasser, S. Bellucci, M. E. Sainio, *Nucl. Phys.* **B423** (1994) 80 and private communication from J. Gasser.

[27] J. A. Oller, L. Roca, *Eur. Phys. J. A* **37** (2008) 15; J. A. Oller, L. Roca, C. Shat, *Phys. Lett.* **B 659** (2008) 2001.

[28] G. Ecker, J. Gasser, A. Pich, E. de Rafael, *Nucl. Phys.* **B321** (1989) 31; *ibid Phys. Lett.* **B 223** (1989) 425.

[29] R. García-Martín and B. Moussalam, *arXiv: 1006.5373 [hep-ph]* (2010).

[30] B. Kniehl and A. Sirlin, *arXiv: 0801.0669 [hep-ph]* (2008).

[31] M. R. Pennington, T. Mori, S. Uehara, Y. Watanabe, *Eur. Phys. J. C* **56** (2008) 1.

[32] J. Bernabeu, J. Prades, *Phys. Rev. Lett.* **100** (2008) 241804.

[33] J. Oller and E. Oset, *Nucl. Phys. A* **629** (1998) 739.

[34] N.N. Achasov, G.N. Shestakov, *Phys. Rev.* **D 77** (2008) 074020.

[35] N.N. Achasov, G.N. Shestakov, *arXiv:0905.2017 [hep-ph]* (2009); N.N. Achasov, A.V. Kiselev, G.N. Shestakov, *Nucl. Phys. Proc. Suppl.* **181-182** (2008) 169;

[36] M. Poppe, *Int. J. Mod. Phys. A* **1** (1986) 545.

[37] M. Feindt, J. Harjes, *Nucl. Phys. B (Proc. suppl.)* **21** (1991) 61

[38] M.A. Shifman, A.I. and Vainshtein and V.I. Zakharov, *Nucl. Phys.* **B147**, 385 (1979).

[39] For a review and references to original works, see e.g., S. Narison, *QCD as a theory of hadrons*, *Cambridge Monogr. Part. Phys. Nucl. Phys. Cosmol.* **17**, 1-778 (2002) [hep-h/0205006]; *QCD spectral sum rules*, *World Sci. Lect. Notes Phys.* **26**, 1-527 (1989); *Acta Phys. Pol.* **B26** (1995) 687; *Riv. Nuov. Cim.* **10N2** (1987) 1; *Phys. Rept.* **84**, 263 (1982).

[40] J. Babcock and J.L. Rosner, *Phys. Rev.* **D 14** (1976) 1286.

[41] S. Narison, *Phys. Lett.* **B 175** (1986) 88.

[42] N.N. Achasov, S.A. Devyanin, G.N. Shestakov, *Z. Phys. C* **16** (1984) 55; N.N. Achasov, G.N. Shestakov, *Phys. Rev. Lett.* **99** (2007) 072001. N.N. Achasov, G.N. Shestakov, *Phys. Rev.* **D 72** (2005) 013006.

[43] A.V. Anisovich et al., *arXiv:hep-ph/0508260* (2005); *Eur. Phys. J. A* **12** (2001) 103; *Phys. Atom. Nucl.* **65** (2002) 497.

[44] V.A. Novikov et al., *Nucl. Phys.* **B 165** (1980) 67.

[45] H.G. Dosch and S. Narison, *Nucl. Phys. Proc. Suppl.* **121** (2003) 114.

[46] H.G. Dosch et al., *hep-ph/0203225*; M. Nielsen et al., *Nucl. Phys. Proc. Suppl.* **121** (2003) 110.

[47] A. Deandrea et al., *arXiv:hep-ph/0012120* (2000).

[48] A. Bramon and S. Narison, *Mod. Phys. Lett. A* **4** (1989) 1113.